Menemui Matematik
(Discovering Mathematics)

journal homepage: https://myjms.mohe.gov.my/index.php/dismath/

MHD Mixed Convection Stagnation-Point Flow over A Vertical Shrinking/Stretching Plate

Siti Fadhilah Mohd Hasyim[1], Fadzilah Md Ali[2*] and Mohd Ezad Hafidz Hafidzuddin[3]

[1,2]*Department of Mathematics and Statistics, Universiti Putra Malaysia, 43400 UPM Serdang, Selangor*
[3]*Centre for Foundation Studies in Science of Universiti Putra Malaysia, Universiti Putra Malaysia, 43400 UPM Serdang, Selangor, Malaysia*

[1]missfadhilahhh@gmail.com, [2]fadzilahma@upm.edu.my, [3]ezadhafidz@upm.edu.my
*Corresponding author

Received: 4 August 2024
Accepted: 24 October 2024

ABSTRACT

The problem of MHD mixed convection stagnation-point flow over a permeable shrinking and stretching plates with the effects of suction and blowing is studied. The effect of viscous dissipation is also being considered. The governing partial differential equations are transformed into an ordinary differential equations via similarity transformations. Using the transformed equations, the numerical results for different parameters are obtained using bvp4c method in Matlab software. For verification, the results are compared with previous published studies, and a good agreement between them are found. In this study, it is observed that the Eckert number increases the skin friction coefficient, however the heat transfer at the surface reduced. For assisting and opposing flows, the velocity pofiles increase with shrinking/stretching parameter. It is found that two solutions observed when assisting and opposing flows are considered, and existing in both shrinking and stretching cases, and also for suction and blowing cases.

Keywords: Mixed Convection, Permeable, Stagnation-Point, Two Solutions

INTRODUCTION

Mixed convection refers to the combination of natural convection and forced convection, occurring when the effects of forced flow in natural convection or buoyant forces in forced convection become significant. Mixed convection is important in many industrial and engineering applications. It plays a crucial role in various industrial and engineering applications, including paper production, steel extrusion, pipeline transport, atmospheric boundary layer flows, electronic power supply, and nuclear reactors. (Yahaya et al., 2023). Khashi'ie et al. (2019) concluded that the fluid velocity increases with magnetic and bouyancy parameters while for the fluid temperature, opposite trends occurred. In mixed convection using hybrid nanofluid model proposed by Zainal et al. (2020), it was found that the fluid velocity increases with magnetic parameter, while the fluid temperature decreases, demonstrating a contradictory behavior. Recently, Mahmood et al. (2024) analyzed three hybrid nanofluid models and concluded that the Xue model yielded the highest average Nusselt numbers, followed by the Yamada-Ota model, and the lowest is the Hamilton-Crosser model.

Some published results based on shrinking and/or stretching plate can be found in Ibrahim et al. (2013), Makinde et al. (2013), Mansur et al. (2015), Jusoh and Nazar (2018), Zainal et al. (2021), Mahabaleshwar et al. (2022), Maranna et al. (2022) and Ul Haq et al. (2023). Ibrahim et al. (2013) analyzed the effect of magnetic field on boundary layer flow and heat transfer of nanofluid over a stretching sheet, observing that the thermal conductivity increased even though there is a small addition of nanoparticles. Other researchers that been cited earlier, namely, Makinde et al. (2013), Mansur et al. (2015), Jusoh and Nazar (2018), Zainal et al. (2021), and Ul Haq et al. (2023) also concentrated on nanofluid model by considering both shrinking sheet and stretching sheet. Recently, many investigations observed multiple solutions specifically two solutions in their study. Two solutions were reported in many research papers, namely in Ali et al. (2014), Mansur et al. (2015), Jusoh and Nazar (2018), Junoh et al. (2021), Zainal et al. (2021), Ul Haq et al. (2023) and many other papers.

The above-mentioned studies assumed that the Eckert number is neglected due to viscous dissipation is small. Not many published papers on Eckert number found in literature. The Eckert number phenomenon is investigated experimentally by Gschwendtner (2004). Gschwendtner (2004) studied the heat transfer from a heated, vertically rotating cylinder subjected to crossflow. Later, Pozzi and Tognaccini (2012) proposed the analytical solution of the laminar incompressible thermo-fluid dynamic field arising in an infinite pipe (circular section) with the effect of Eckert number. Further, Kejela et al. (2021) solved the problem of magnetohydrodynamic (MHD) Hiemenz flow by using optimal homotopy asymptotic method and found that the temperature of the fluid increases with the Eckert number, however the velocity of the fluid is not affected by the Eckert number. Ramzan et al. (2021) employed the homotopy analysis method (HAM) and observed unique solution. Ramzan et al. (2021) considered both slip and no-slip conditions, and observed that the Nusselt number and skin friction coefficient increased with Eckert number, stretching parameter, heat generation parameter and radiation parameter. Later, Dessie (2021) applied the scaling group transformation method to convert the partial differential equations into a system of nonlinear ordinary differential equations and concluded that the Eckert number leads to a decrease in the fluid temperature in the thermal boundary layer region of the Casson fluid flow.

Recently, Jabeen et al. (2024) solved numerically the problem involving Williamson nanofluid with the presence of viscous dissipation, bioconvection and activation energy. Further, in the problem of mixed convection boundary layer flow over a horizontal circular cylinder in hybrid nanofluid, Elfiano et al. (2024) solved numerically the transformed partial differential equations using Keller-box method. Elfiano et al. (2024) observed that the Eckert number has decreased the temperature distribution with no significant change in the fluid velocity and concluded that the viscous dissipation effect was minimal at stagnation region. To date, not much research done related to viscous dissipation. Hence, the recent literatures are hard to find.

The problem of MHD stagnation-point flow and heat transfer over a permeable shrinking plate and stretching plate investigated by Ali et al. (2014) and observed that the Eckert number reduced the heat transfer rate at the surface, and two solutions found to exist for both suction and injection cases. Therefore, the aim of this present paper is to extend the research performed by Ali et al. (2014) by considering the bouyancy effect on MHD mixed convection boundary layer flow over a vertical permeable plate. We also consider shrinking plate and stretching plate, as well as the effect of viscous dissipation.

MATHEMATICAL FORMULATION

Consider a steady MHD two-dimensional stagnation-point flow of a viscous, incompressible electrically conducting fluids over a vertical permeable flat plate such that the plate is shrinking or stretching in its own plane with the effects of an externally applied magnetic field with constant strength, H_0 and viscous dissipation.

It is assumed that both the shrinking/stretching velocity, $u_w(x)$ and the external velocity, $u_e(x)$ impinging the stretching plate vary linearly with the distance from the stagnation-point, namely $u_w(x) = mx$ and $u_e(x) = px$, where p and m are constants with $p > 0$, and $m < 0$ for shrinking plate and $m > 0$ for stretching plate. It is also assumed that the velocity of the mass flux is v_0, where $v_0 < 0$ represents suction and $v_0 > 0$ represents blowing. We also assume that the surface temperature varies with the distance from the stagnation-point such that $Tr_w(x) = Tr_\infty + kx^2$ where Tr_w is surface temperature, Tr_∞ is the ambient temperature and k is a positive constant with $k > 0$ for a heated surface $Tr_w(x) > Tr_\infty$ (assisting flow) and $k < 0$ for a cooled surface $Tr_w(x) < Tr_\infty$ (opposing flow). When the upper half of the plate is heated and the lower half of the plate is cooled, the assisting flow occurs. Meanwhile, opposing flow occurs when the upper section of the plate is cooled while the lower section is heated.

Therefore, the basic governing equations are

$$\frac{\partial u}{\partial x} + \frac{\partial v}{\partial y} = 0 \tag{1}$$

$$u\frac{\partial u}{\partial x} + v\frac{\partial u}{\partial y} = u_e\frac{du_e}{dx} + \nu\frac{\partial^2 u}{\partial y^2} + \frac{\sigma_e u_e^2 H_0^2}{\rho}(u_e - u) + g\beta(Tr - Tr_\infty) \tag{2}$$

$$u\frac{\partial Tr}{\partial x} + v\frac{\partial Tr}{\partial y} = \alpha\frac{\partial^2 Tr}{\partial y^2} + \frac{\nu}{C_s}\left(\frac{\partial u}{\partial y}\right)^2 + \frac{\sigma_e \mu_e^2 H_0^2}{\rho C_p}(u_e - u)^2 \tag{3}$$

where u and v are the velocity components along the x and y axes, respectively. Further, ρ is the fluid density, C_s is specific heat capacity at constant pressure, Tr is the fluid temperature, ν is the kinematic viscosity, μ_e is magnetic permeability, g is the gravity acceleration, σ_e is the electrical conductivity, β is the thermal expansion coefficient and α is the thermal diffusivity.

Following Ali et al. (2014), the boundary conditions for Eqs. (1) - (3) are

$$v = v_w(x) = v_0,\ u = u_w(x) = mx\ , Tr = Tr_w(x) = Tr_\infty + kx^2 \ \text{ at } y = 0 \tag{4}$$

$$u = u_e(x) \to px,\ Tr \to Tr_\infty \qquad \text{as } y \to \infty. \tag{5}$$

The nonlinear partial differential Eq. (1) is satisied, while Eqs. (2) and (3) are transformed into nonlinear ordinary differential equations using the following similarity transformation:

$$\psi = x\sqrt{p\nu}f(\eta),\ \theta(\eta) = \frac{Tr - Tr_\infty}{Tr_w - Tr_\infty},\ \eta = \sqrt{\frac{p}{\nu}}y \tag{6}$$

where ψ is the stream function, with $u = \frac{\partial\psi}{\partial y}$ and $v = -\frac{\partial\psi}{\partial x}$. Thus, using Eq. (6), Eqs. (2) and (3) are reduced to the following set of ordinary differential equations:

$$f''' + ff'' + 1 - f'^2 + M^2(1 - f') + \lambda\theta = 0 \tag{7}$$

$$\frac{1}{Pr}\theta'' + f\theta' - 2f'\theta + Ecf''^2 + EcM^2(1 - f')^2 = 0. \tag{8}$$

By applying the similarity transformation (6) to Eqs. (4) and (5), we obtain a new set of boundary conditions as follows:

$$f(0) = s,\ f'(0) = A,\ \theta(0) = 1 \tag{9}$$

$$f'(\eta) \to 1\,, \theta(\eta) \to 0 \ \text{ as } \eta \to \infty \tag{10}$$

with primes denote differentiation with respect to η, $M = \mu_e H_0 \sqrt{\frac{\sigma_e}{a\rho}}$ is the magnetic parameter, $\Pr = \frac{\nu}{\alpha}$ is the Prandtl number, $Ec = \frac{u_e^2(x)}{C_s[Tr_w(x) - Tr_\infty]}$ is the Eckert number, $s = -\frac{\nu_0}{\sqrt{p\nu}}$ is the mass flux parameter, $A = \frac{m}{p}$ is the shrinking/stretching parameter and $\lambda = \frac{Gr_x}{Re_x^2}$ is the mixed convection parameter (also known as bouyancy parameter), where $Gr_x = g\beta(Tr_w - Tr_\infty)x^3/\nu^2$ is the local Grashof number and $Re_x = u_e(x)x/\nu$ is the local Reynolds number.

It is good to mention that $A < 0$ represents a shrinking plate, $A > 0$ represents a stretching plate and for a fixed plate, $A = 0$. Noticed that $\lambda < 0$ corresponds to opposing flow and $\lambda > 0$ corresponds to an assisting flow. Meanwhile, $s < 0$ and $s > 0$ are refer to blowing case and suction case, respectively.

The physical quantities in this study are the local skin friction coefficient and local Nusselt number given by

$$C_f = \frac{\tau_w}{\rho u_e^2(x)}\,, \quad Nu_x = \frac{x q_w}{c(Tr_w - Tr_\infty)} \tag{11}$$

where $\tau_w = \mu \left(\frac{\partial u}{\partial y}\right)_{y=0}$ is the wall shear stress along the surface and $q_w = -c\left(\frac{\partial Tr}{\partial y}\right)_{y=0}$ is the surface heat flux, with μ is the dynamic viscosity and c is the thermal conductivity. Using Eq. (6), Eq. (11) becomes

$$C_f\, Re_x^{\frac{1}{2}} = f''(0), \quad Re_x^{-1/2} Nu_x = -\theta'(0). \tag{12}$$

RESULTS AND DISCUSSION

The numerical results obtained by solving the transformed equations (7) and (8) together with the new boundary conditions (9) and (10) using bvp4c in Matlab solver. By using bvp4c, we will obtain the velocity profiles, temperature profiles, the skin friction coefficient and local Nusselt number for various values of parameters, namely, the stretching/shrinking parameter A, magnetic parameter M, mass flux parameter s, Prandtl number Pr, Eckert number Ec, and bouyancy parameter λ. Following Gschwendtner (2004), maximum heat transfer occurs when the Eckert number (Ec) is approximately 0.3. Thus, for this study, we adopt $Ec = 0.3$.

To ensure the validity and accuracy of this present method, the numerical results of the dimensionless skin friction coefficient $f''(0)$ and the local Nusselt number $-\theta'(0)$ obtained are being compared with those of Ishak et al. (2010) and Ali et al. (2014), where two solutions are produced. Therefore, Table 1 displays the numerical comparison results of the skin friction coefficient $f''(0)$ for different values of shrinking/stretching parameter A, when the magnetic parameter M, Eckert number Ec, the mass flux parameter s and the bouyancy parameter λ are absent. From Table 1, it is found that the results of this present research and previous published papers are in very good agreement for skin friction coefficient. The table also shows the two solutions occur when the plate is shrunk and unique solution found for stretching case.

Table 1: Comparison values for skin friction coefficient for stretching and shrinking cases when $M = 0$, $Ec = 0$, $s = 0$ and $\lambda = 0$. Results in [ ] refer to the second solution

	$f''(0)$		
A	Ishak et al. (2010)	Ali et al. (2014)	Current Results
0	1.232588	1.232588	1.232588
0.5	0.713295	0.713295	0.713295
1	0	0	0
–0.5	1.495670	1.495670	1.495670
−1	1.328817	1.328817	1.328817
−1.15	1.082231	1.082231	1.082231
	[0.116702]	[0.116702]	[0.116702]
−1.2465	0.554283	0.554283	0.554283
	[0.584295]	[0.584295]	[0.584295]

Figures 1 and 2 demonstrate the effect of shrinking/stretching parameter on velocity profile for assisting and opposing flows, respectively. Figures 1 and 2 show that the velocity profiles increase as A increases in first solution. For second solution, the velocity profile of Figures 1 and 2 displays an uncertainty trend with A. Figure 3 shows the influence of shrinking/stretching parameter on temperature profiles. The temperature profiles are not very significant, as can be seen for the first solution.

While, Figures 4 and 5 show the impact of bouyancy parameter on the velocity profiles and temperature profiles, respectively. For the first solution, the velocity profiles increase with λ, however the second solution shows opposite effect after a certain point. Increasing the values of λ has the effect of thinning the boundary layer. Meanwhile, Figure 5 demonstrates the temperature profiles for both assisting and opposing flows. Figures 1-5 depict there exist two velocity profiles and temperature profiles. Thus, two solutions exist for assisting and opposing flows and occurred when the plate is stretch and shrunk. It is evident from Figures 1-5 that the boundary layer thickness for the first solution is consistently thinner than that of the second solution, with both profiles approaching the boundary conditions (8) asymptotically as $n \to \infty$.

The skin friction coefficient $f''(0)$ and the heat transfer rate at the surface (also known as the local Nusselt number) $-\theta'(0)$ against the stretching/shrinking parameter A with different values of the mass flux parameter s, for assisting flow and opposing flow, respectively, are shown in Figures 6 and 7. Figures 6 and 7 also discover two solutions for both suction and blowing cases, and shrinking and stretching cases. The effect of A has increased the skin friction coefficient $f''(0)$ and after reached certain points of parameter A, $f''(0)$ decreases. At the same time, the skin friction coefficient $f''(0)$ for the first solution increases alongside the values of mass flux parameter s. The reason is that mass flux parameter creates more resistance to the transport phenomena. Therefore, s increases the local Nusselt number. This can be seen clearly from Figure 7. The shrinking and stretching parameter also found to increase the heat transfer rate at the surface. From Figures 6 and 7, it is found that blowing accelerates the boundary layer separation from the wall.

Meanwhile, Figures 8 and 9 show the influence of mass flux parameter, s and Eckert number, Ec on the skin friction coefficient $f''(0)$ and the local Nusselt number, $-\theta'(0)$, respectively. Both Figures 8 and 9 show the existence of two solutions for various values of mass flux parameter and the Eckert number. Figures 8 shows the skin friction coefficient increase as the value of Ec and s increases, for first solution. For second solution, opposite phenomenon occurs for Ec, however, the skin friction coefficient increases with s, then decreases after a certain point. On the other hand, for the local Nusselt number as displayed in Figure 9, opposite effects discover for the first and second solutions. Interesting result from Figure 9 is that the upper branch demonstrates the second solution and lower branch demonstrates the first solution. In many cases, the upper branch always refers to the first solution and vice versa. This can be validated through a stability analysis. However, such analysis is not reported in this study.

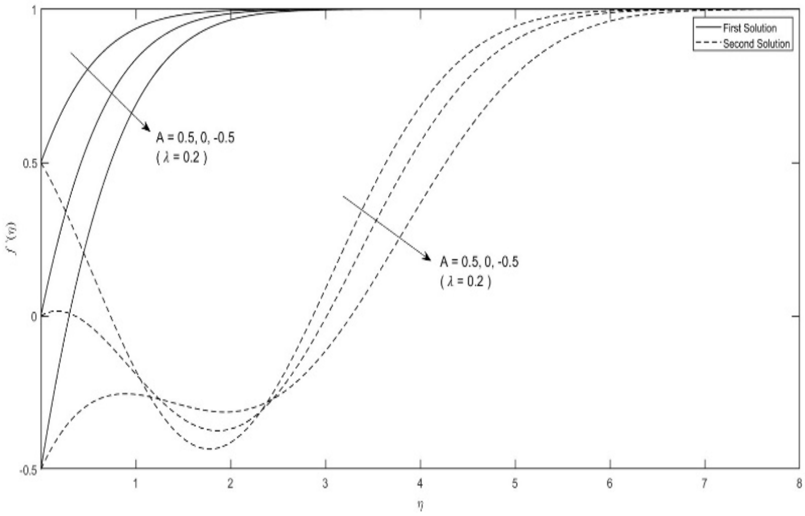

Figure 1: Velocity profiles for various values of A when s = 0.3, Ec = 0.2, M = 0.2, Pr = 1 and λ = 0.2

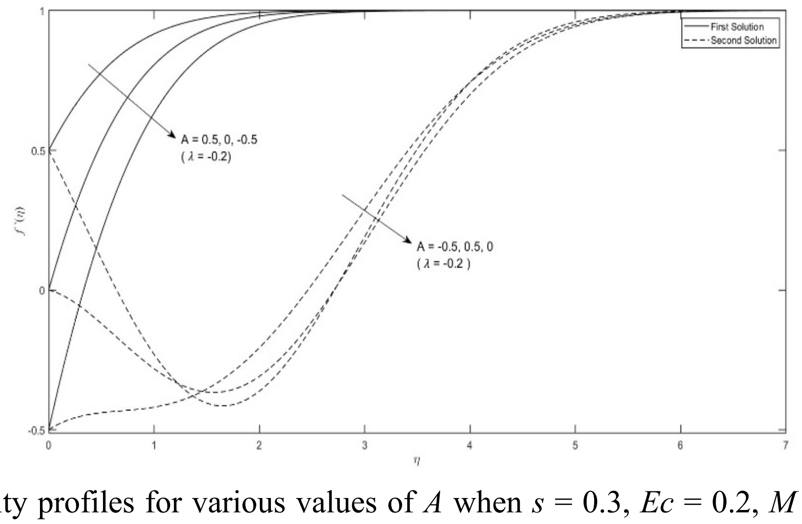

Figure 2: Velocity profiles for various values of A when s = 0.3, Ec = 0.2, M = 0.2, Pr = 1 and $\lambda = -0.2$

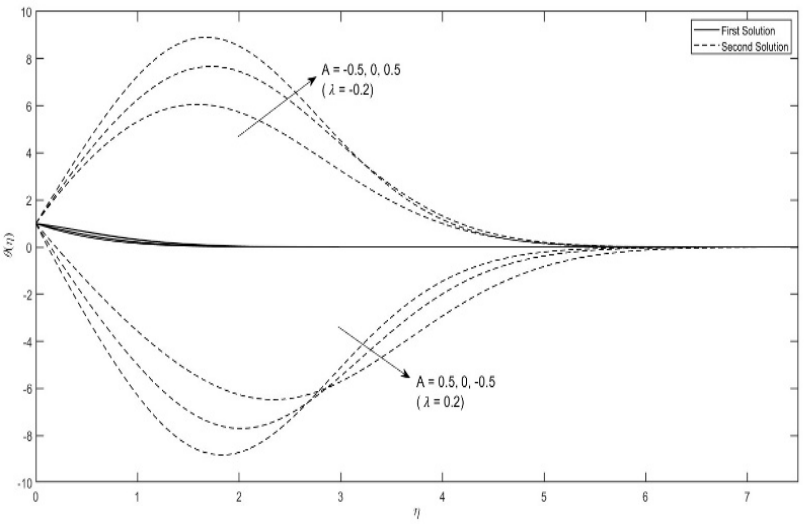

Figure 3: Temperature profiles for various values of A when s = 0.3, Ec = 0.2, M = 0.2, Pr = 1 and λ = 0.2, −0.2

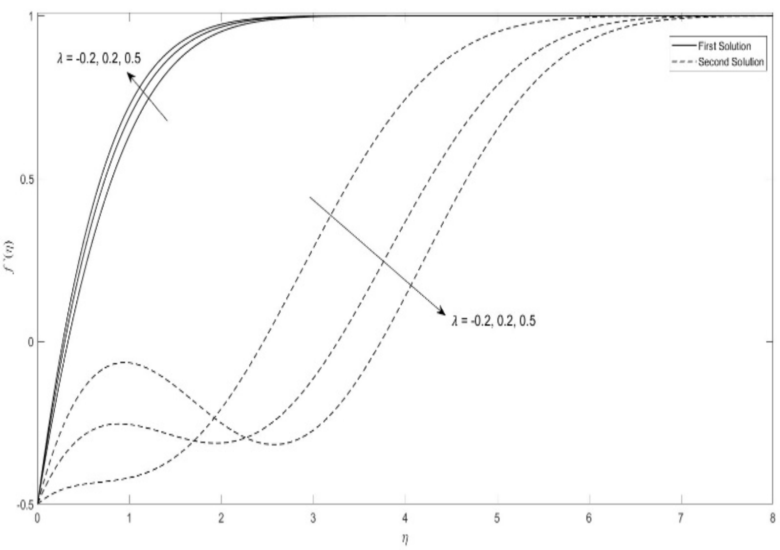

Figure 4: Velocity profiles for various values of λ when s = 0.3, A = −1.3, M = 0.2, Pr = 1 and Ec = 0.2

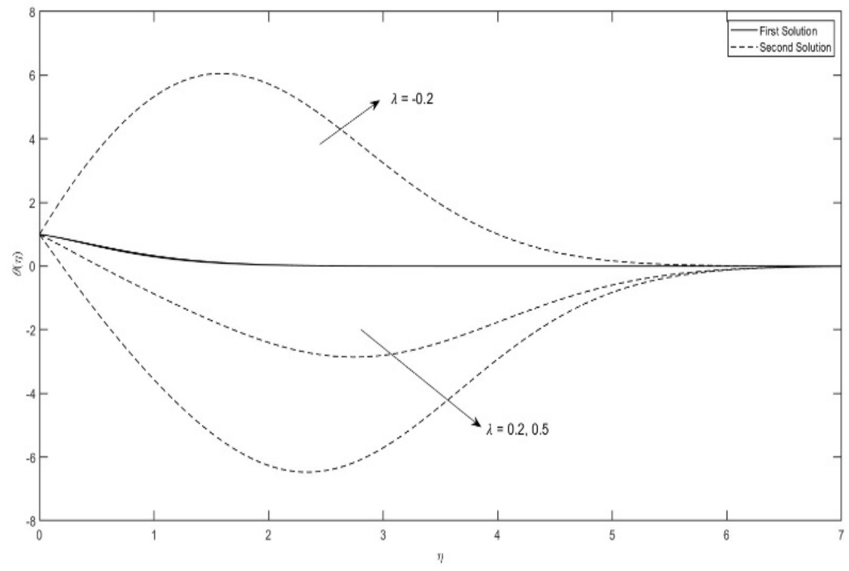

Figure 5: Temperature profiles for various values of λ when $s = 0.3$, $A = -1.3$, $M = 0.2$, $\Pr = 1$ and $Ec = 0.2$

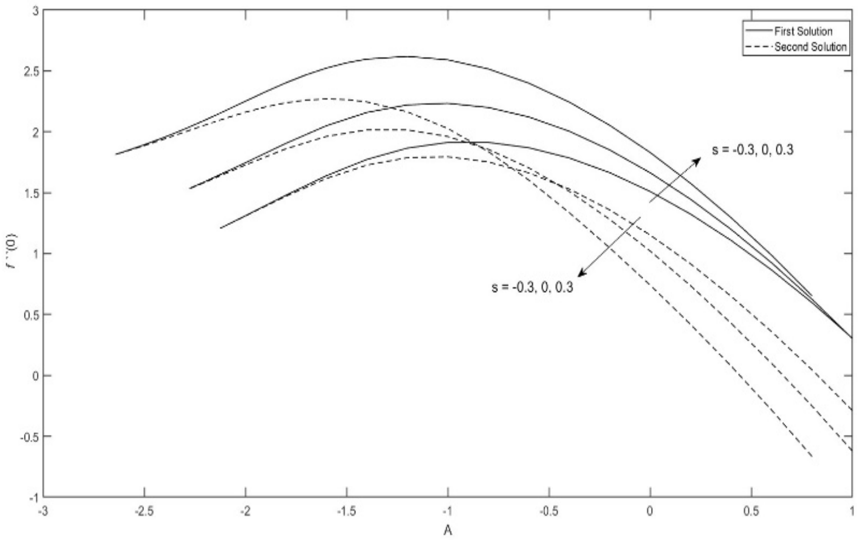

Figure 6: The skin friction coefficient $f''(0)$ with A for various values of s and fixed $\lambda = 1$, $\Pr = 1$, $Ec = 0.2$ and $M = 0.2$

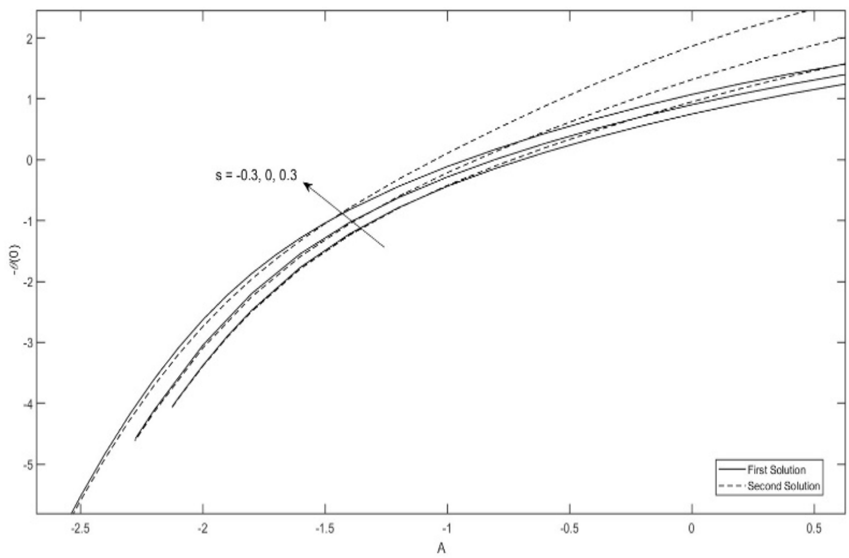

Figure 7: The local Nusselt number $-\theta'(0)$ with A for various values of s and fixed $\lambda = 1$, Pr = 1, $Ec = 0.2$ and $M = 0.2$

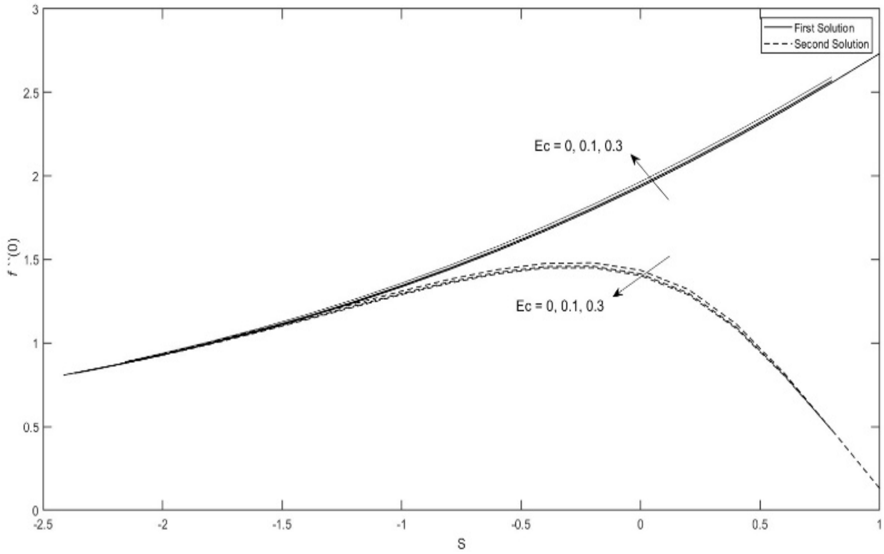

Figure 8: The skin friction coefficient $f''(0)$ with s for various values of Ec and fixed $A = -0.5$, Pr = 1, $\lambda = 1$ and $M = 0.2$

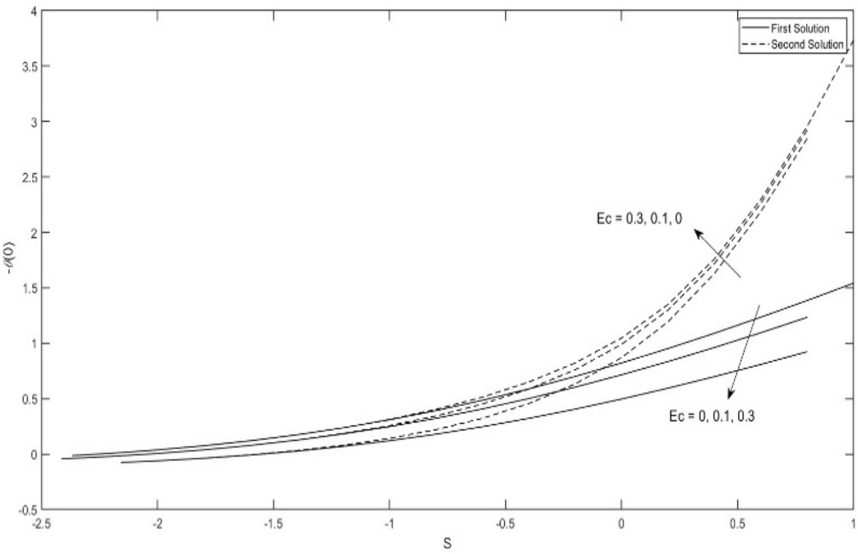

Figure 9: The local Nusselt number $-\theta'(0)$ with s for various values of Ec and fixed $A = -0.5$, $\Pr = 1$, $\lambda = 1$ and $M = 0.2$

CONCLUSION

In this paper, the problem of MHD mixed convection stagnation-point flow and heat transfer over a permeable shrinking/stretching plate is solved numerically using bvp4c method. The current results are compared with previous studies, and it gives a favorable agreement. The main findings are summarized as follows:

- The velocity profiles increase with bouyancy parameter in first solution and opposite effect found for second solution.
- The Eckert number increases the skin friction coefficient, however reduced the surface heat transfer.
- Mass transfer parameter increase the skin friction coefficient (for upper branch), as well as the local Nusselt number (for upper and lower branches).
- Multiple solutions (namely two solutions) are observed for
  - assisting and opposing flows,
  - shrinking and stretching cases,
  - suction and blowing cases.
- Blowing accelerates the boundary layer separation from the wall.

REFERENCES

Ali, F.M., Nazar, R., Arifin, N., and Pop, I. (2014). MHD Stagnation-Point Flow and Heat Transfer over a Permeable Stretching/Shrinking Sheet. In AIP *Conference Proceedings*, **1602**: 125–131.

Dessie, H. (2021). MHD stagnation point flow of Casson fluid over a convective stretching sheet considering thermal radiation, slip condition, and viscous dissipation. *Heat Transfer,* 50(7): 6984-7000

Elfiano, E., Nik Ibrahim, N. M. I. and Mohamed, M. K. A. (2024). Mixed Convection Boundary Layer Flow over a Horizontal Circular Cylinder in Al_2O_3/Water Hybrid Nanofluid with Viscous Dissipation. *CFD Letters*, **16(4)**: 98-110.

Gschwendtner, M. A., (2004). The Eckert Number Phenomenon: Experimental Investigations on the Heat Transfer from a Moving Wall in the Case of a Rotating Cylinder. *Heat Mass Transf.*, **40**:551-559.

Ishak, A., Lok, Y. Y. and Pop, I. (2010). Stagnation-point flow over a shrinking sheet in a micropolar fluid. *Chemical Engineering Communications*, **197(11)**: 1417–1427.

Ibrahim, W., Shankar, B. and Nandeppanavar, M. M. (2013). MHD Stagnation-Point Flow and Heat Transfer due to Nanofluid Towards a Stretching Sheet. *International Journal of Heat and Mass Transfer*, **56**: 1–9.

Jabeen, K., Mushtaq, M., Mushtaq, T. and Muntazir, R. M. A. (2024). A Numerical Study of Boundary Layer Flow of Williamson Nanofluid in the Presence of Viscous Dissipation, Bioconvection and Activation Energy. *Numerical Heat Transfer, Part A: Applications,* **85(3)**: 378-399.

Junoh, M. M., Abdullah, N. and Ali, F. M. (2021). Dual Solutions of MHD Stagnation Slip Flow Past a Permeable Plate. *Journal of Advanced Research in Fluid Mechanics and Thermal Sciences*, **80(1)**: 137-146.

Jusoh, R. and Nazar, R. (2018). MHD Stagnation-Point Flow and Heat Transfer of a Nanofluid over a Permeable Nonlinear Stretching/Shrinking Sheet with Viscous Dissipation Effect. In *AIP Conference Proceedings* (Vol. **1940**).

Kejela S. B., Daba, M. and Girum, A. (2021). Investigation of Effects of Thermal Radiation, Magnetic Field, Eckert Number, and Thermal Slip on MHD Hiemenz Flow by Optimal Homotopy Asymptotic Method. *Journal of Mathematics Volume*, **2021**: Article ID 5590657, 15 pages.

Khashi'ie, N. S. Arifin, N. M., Hafidzuddin, E. H. and Wahi, N. (2019). MHD Mixed Convective Stagnation Point Flow with Heat Generation Past a Shrinking Sheet. *ASM Science Journal*, **12**: 71-81.

Mahabaleshwar, U. S., Sneha, K. N., Chan, A. and Zeidan, D. (2022). An Effect of MHD Fluid Flow Heat Transfer Using CNTs with Thermal Radiation and Heat Source/Sink Across a Stretching/Shrinking Sheet. *International Communications in Heat and Mass Transfer*, **135**: 106080.

Mahmood, Z., Rafique, K., Khan, U., Adnan, El-Rahman, M. A. and Rabab Alharbi, R. (2024). Analysis of Mixed Convective Stagnation Point Flow of Hybrid Nanofluid over Sheet with Variable Thermal Conductivity and Slip Conditions: A Model-Based Study. *International Journal of Heat and Fluid Flow*, **106**: 109296.

Makinde, O. D., Khan, W. A. and Khan, Z. H. (2013). Buoyancy Effects on MHD Stagnation-Point Flow and Heat Transfer of a Nanofluid Past a Convectively Heated Stretching/Shrinking Sheet. *International Journal of Heat and Mass Transfer*, **62**: 526–533.

Mansur, S., Ishak, A., and Pop, I. (2015). The Magnetohydrodynamic Stagnation-Point Flow of a Nanofluid over a Stretching/Shrinking Sheet with Suction, PLoS One, **10 (3)**: e0117733.

Maranna, T., Sneha, K. N., Mahabaleshwar, U. S., Sarris, I. E. and Karakasidis, T. E. (2022). An Effect of Radiation and MHD Newtonian Fluid over a Stretching/Shrinking Sheet with CNTs and Mass Transpiration. *Appl. Sci.*, **12(11)**: 5466.

Pozzi, A., and Tognaccini, R. (2012). The Effect of the Eckert Number on Impulsively Started Pipe Flow. *European Journal of Mechanics B/Fluids*, **36**: 120-127.

Ramzan, M. Dawar, A. Anwar Saeed, A., Kumam P., Watthayu, W. and Kumam, W., (2021), Heat Transfer Analysis of the Mixed Convective Flow of Magnetohydrodynamic Hybrid Nanofluid Past a Stretching Sheet with Velocity and Thermal Slip Conditions, *Plos One*, **16(12)**: e0260854.

Ul Haq, R., Zahoor Z. and Shah, S. S. (2023). Existence of Dual Solution for MHD Boundary Layer Flow over a Stretching/Shrinking Surface in the Presence of Thermal Radiation and Porous Media: KKL Nanofluid Model. *Heliyon*, **9**: e20923.

Yahaya, R. I., Arifin, N. M., Pop, I., Ali, F. M. and Isa, S. S. P. M. (2023). Dual Solutions of Unsteady Mixed Convection Hybrid Nanofluid Flow Past a Vertical Riga Plate with Radiation Effect, *Mathematics*, **11**: 215.

Zainal, N. A., Nazar, R., Naganthran, K. and Pop, I. (2020). MHD Mixed Convection Stagnation Point Flow of a Hybrid Nanofluid Past a Vertical Flat Plate with Convective Boundary Condition. *Chinese Journal of Physics*, **66**: 630-644.

Zainal, N. A., Nazar, R., Naganthran, K. and Pop, I. (2021). Unsteady MHD Stagnation Point Flow Induced by Exponentially Permeable Stretching/Shrinking Sheet of Hybrid Nanofluid. *Engineering Science and Technology, an International Journal*, **24(5)**: 1201-1210.